Chapter 3

Modelling precipitation reactions in steels

The formation of an individual particle involves its nucleation and growth. A good thermodynamic description of the phases involved is essential in order to model the kinetics of this reaction. For this reason, this chapter includes a presentation of the CALPHAD method on which are built the SGTE databases used in thermodynamic calculation software such as MT-DATA or ThermoCalc; it then introduces physical models for nucleation and growth. The overall precipitation process must also account for impingement effects. This can be dealt with using the theory for overall transformation kinetics as first expressed by Kolmogorov [78], Johnson and Mehl [79], and Avrami [80].

3.1 Thermodynamic models for solution and compound phases

The use of phase-diagrams has, for long, been seen as being rather academic, because most real materials are multicomponent in nature, while phase diagrams are generally used to represent binary or ternary systems.

The CALPHAD (CALculation of PHAse Diagram) method has altered this viewpoint because it is now possible to predict the phase behaviour of complex, multicomponent systems, based on the extrapolation of thermodynamic properties. At the heart of this method is the calculation of the Gibbs energy of a phase as a function of its composition, temperature and pressure. Once this is possible, the problem of predicting an equilib-

rium is essentially mathematical, although far from simple given the number of variables involved in the minimisation process.

The models in use for the Gibbs energy vary with the nature of the phase considered. The following introduces the problem for pure substances, solutions and sublattice phases, which are the most commonly used in the field of metallurgy. The phases of interest in the present work fall into three categories: MX precipitates (TiN, NbN, *etc.*) are modelled as pure substances, complex carbides (e.g. $M_{23}C_6$, M_6C) and austenite are sublattice phases, while the liquid phase is a random substitutional solution.

The following is essentially based on references [81, 82, 83].

3.1.a Pure substances

For a stoichiometric compound, it is sufficient to know the heat capacity together with reference values to obtain the Gibbs energy at any temperature. The SGTE (Scientific Group Thermodata Europe) databases store the coefficients for the heat capacity at constant pressure, C_P, written as a polynomial of temperature:

$$C_P(T) = A + BT + CT^2 + DT^{-2} \tag{3.1}$$

together with values for $\Delta_f H$, the enthalpy of formation of the substance, and S_{298} the entropy at 298 K. The coefficients are valid only within a given range of temperature, and the database provides parameters as a function of temperature interval.

3.1.b Random substitutional solutions

In random substitutional solutions, such as gas, or simple metallic liquid and solid solutions, the components can mix on any spatial position available to the phase. The Gibbs energy of a solution is traditionally decomposed according to:

$$G = G^\circ + G^{ideal}_{mix} + G^{xs}_{mix} \tag{3.2}$$

where G° is the contribution of the pure components, G^{ideal}_{mix} the ideal mixing contribution and G^{xs}_{mix} the deviation from ideality also known as excess Gibbs energy of mixing.

i Ideal solutions

This is the simplest possible case. The interactions between the different elements are identical and there is no enthalpy change when the solution is formed. The only

contribution to the Gibbs energy change is due to the increase of configurational entropy. This term can be simply calculated using Stirling's approximation for large factorials.

$$\Delta S_{\text{random}} = -R \sum_i (x_i \ln x_i) \tag{3.3}$$

where x_i is the atomic fraction of component i and R the gas constant. The Gibbs energy per mole of solution is therefore:

$$G = \sum_i x_i G_i^\circ + RT \sum_i x_i \ln x_i \tag{3.4}$$

ii Regular and non-regular solutions

In most cases however, there are interactions between the components of a phase. In the case of a binary system AB, the regular model assumes the total energy of solution can be written :

$$E = N_{AA}\varepsilon_{AA} + N_{BB}\varepsilon_{AA} + N_{AA}N_{AB}\varepsilon_{AB} \tag{3.5}$$

where N_{AA} is the number of AA pairs, and ε_{AA} their bond energy, it can be shown that the enthalpy of mixing is:

$$\Delta H_{mix} = \frac{Nz}{2} x(1-x)\left(2\varepsilon_{AB} - \varepsilon_{AA} - \varepsilon_{BB}\right) \tag{3.6}$$

where N is the number of atoms in solution, and z the coordination number of the structure, that is the number of nearest neighbours of any atom.

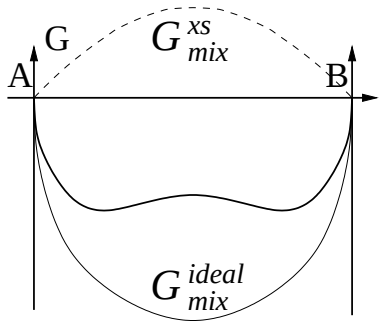

Figure 3.1: Modification introduced by the regular term: this diagram shows the Gibbs energy of mixing with its two contributions as a function of x. If $T < \omega/2R$, the curve has two points of inflection between which there is a miscibility gap; this is the case illustrated here.

For a regular solution, it is also assumed that the entropy of mixing is as given by equation 3.3 so that it does not contribute to the excess Gibbs energy of mixing , therefore G^{xs}_{mix} is:

$$G^{xs}_{mix} = \omega x(1-x) \tag{3.7}$$

where $\omega = Nz/2(2\varepsilon_{AB} - \varepsilon_{AA} - \varepsilon_{AA})$ is a temperature dependent parameter on which depends the behaviour of the solution (figure 3.1). Generalised to a multicomponent random solution, the Gibbs energy per mole is written:

$$G = \sum_i x_i G^\circ_i + RT \sum_i x_i \ln x_i + \sum_i \sum_{j>i} x_i x_j \omega_{ij} \tag{3.8}$$

However, this assumes interactions to be composition independent, which is not realistic in most cases. The sub-regular model, proposed by Kaufman and Berstein, introduces a linear composition dependency and expresses the excess Gibbs energy of mixing as:

$$G^{xs}_{mix} = \sum_i \sum_{j>i} x_i x_j (\omega^i_{ij} x_i + \omega^j_{ij} x_j) \tag{3.9}$$

This is generalised to any composition dependency in the Redlich-Kister power series, which expresses G^{xs}_{mix} as:

$$G^{xs}_{mix} = \sum_i \sum_{j>i} x_i x_j \sum_v \omega^v_{ij} (x_i - x_j)^v \tag{3.10}$$

In the SGTE databases, the individual parameters ω are written:

$$\omega = A + BT + CT\ln T + DT^2 \tag{3.11}$$

and these coefficients are stored for each ω^v_{ij}.

3.1.c Sublattice models

The different expressions for G^{xs}_{mix} presented above are all for solutions where the components can mix freely on the sites available for the phase. In many cases, however, different components mix on different sublattices, as with austenite, where C, N, B mix on the interstitial sublattice, while Fe, Cr, Ni, *etc.* mix on the substitutional one. For a two-sublattice phase, with A and B on the first sublattice, C and D on the second, considering a regular solution, the excess Gibbs energy of mixing is written:

$$G^{xs}_{mix} = y^1_A y^1_B L^\circ_{A,B:*} + y^2_C y^2_D L^\circ_{*:C,D} \tag{3.12}$$

where $L^{\circ}_{A,B:*}$ and $L^{\circ}_{*:C,D}$ are regular solution parameters for mixing on the sublattices irrespective of site occupation of the other sublattice. The mole fractions (e.g. x_A) are now replaced by the occupied site fractions (y^1_A, where 1 denotes the first sublattice). A sub-regular model is introduced by making the interactions dependent on the site occupation of the other sublattice, as:

$$\begin{aligned} G^{xs}_{mix} &= y^1_A y^1_B y^2_C \, L^{\circ}_{A,B:C} + y^1_A y^1_B y^2_D \, L^{\circ}_{A,B:D} \\ &\quad + y^2_C y^2_D y^1_A \, L^{\circ}_{A:C,D} + y^2_C y^2_D y^1_B \, L^{\circ}_{B:C,D} \end{aligned} \tag{3.13}$$

The temperature dependency is obtained by writing the parameters $L^{\circ}_{A,B:C}$ as polynomials of T and $\ln T$, and it is the coefficients of these polynomials which are stored in the SGTE databases.

3.1.d The SGTE databases

The purpose of this section is to describe the limitations of the SGTE databases when dealing with systems such as NF709 (composition in table 1.1). These limitations can be classified in three categories:

- Absence of a phase: this is the case of Z-phase and G-phase for which no information is present in the database.
- Absence of an element within a phase, for example, Nb is not included in M_6C in the databases.
- Absence of parameters: an element can be allowed to enter a phase, but there is no information about its interactions with the other elements. For example, there is no parameter for Nb and N interactions in austenite. When this arises for two elements on a same sublattice, they are modelled as an ideal solution.

i Missing Phases

Two phases reported to form in austenitic stainless steels are not present in the SGTE databases. Z-phase, which forms in the early stages of precipitation in nitrogen-bearing stabilised austenitic stainless steels, and G-phase, which is sometimes reported in 20/25 niobium stabilised steels, after long-term ageing.

ii Missing Solubilities

For many phases, not all the elements which are known to dissolve in the phase are found in the database. In the following table, the substitutions reported in literature are reported, and the substitutions allowed by the SGTE are compared.

Phase	Elements reported in literature	Elements allowed by SGTE
$M_{23}C_6$	Cr Fe Mo C Mn Ni P B N	Cr Fe Mn Ni Mo C
M_6C	Fe Cr Mo Si Nb Ti Ni C N	Fe Cr Mo C
Sigma	Fe Cr Ni Mo Mn	Fe Cr Ni Mo Mn
Laves phase	Fe Ti Nb Mo	Fe Ti Nb Mo

iii Missing Parameters

There are more than 800 parameters missing for the description of all the phases able to form in a system corresponding to NF709. Although some have no importance because they describe phases which are not expected to form, it is difficult to judge of the consequences of most of them. In austenite, for example, most of the interaction parameters for boron with other elements are missing. However, boron may be present in very small quantities. A number of parameters are also missing for niobium and it is more difficult to estimate the consequences.

3.2 The classical theory for nucleation

In this section the main lines of the derivation of nucleation rate as calculated in classical theory are given, together with modifications for nucleation on dislocations, on grain boundaries and for non-spherical shapes.

3.2.a Nucleation rate in the classical theory

At any temperature above absolute zero, composition and structure fluctuations constantly occur in alloys as a result of thermal agitation. These fluctuations can lead to the formation of stable nuclei of a new phase.

In classical theory, the probability P of a fluctuation giving a nucleus leading to an increase of Gibbs energy ΔG is calculated according to the Boltzmann statistics:

$$P(\Delta G) = A \exp\left(\frac{-\Delta G}{RT}\right)$$

Although the nucleus is extremely small, macroscopic thermodynamical variables are used to give an expression for ΔG, because the rate is an average function. Considering the formation of a nucleus of θ in a matrix γ, r being the radius of the nucleus, the change in Gibbs energy is:

$$\Delta G = \frac{4\pi r^3}{3}\Delta G_v + 4\pi r^2 \sigma_{\gamma\theta} \tag{3.14}$$

where $\sigma_{\gamma\theta}$ is the interface energy per unit area between the two phases, and ΔG_v is the Gibbs energy change per unit volume of embryo.

The change in Gibbs energy shows two contributions which act in opposition. In this case, the Gibbs energy change decreases with increasing size only above a critical radius r_c. The critical radius and the activation energy G^* are, assuming a spherical nucleus and

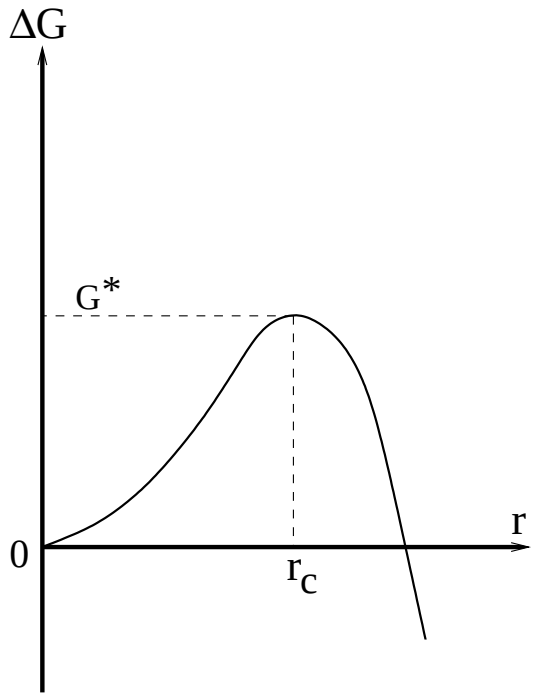

Figure 3.2: Schematic variation of the Gibbs energy change with the size of a nucleus in a supersaturated solution. After [84].

neglecting possible strain effects:

$$r_c = -\frac{2\sigma_{\gamma\theta}}{\Delta G_v} \quad \text{and} \quad G^* = \frac{16\pi}{3}\frac{{\sigma_{\gamma\theta}}^3}{{\Delta G_v}^2} \tag{3.15}$$

The nucleation rate is then derived by considering the frequency with which an atom adds

to a critical radius and makes it stable:

$$I = N \exp\left(-\frac{G^*}{RT}\right) \nu \exp\left(-\frac{G_t^*}{RT}\right) \tag{3.16}$$

where ν is an attempt frequency, often taken as being kT/h, N a number density of nucleation sites and G_t^* the activation energy for transfer of atoms across the $\gamma\theta$ interface.

3.2.b Heterogeneous nucleation

Homogeneous nucleation very seldom occurs in solid-state transformations. The presence of defects, with which is associated a given energy, provides sites for preferential nucleation. In austenitic stainless steels, MX carbides nucleate intragranularly on dislocations, and most of the other carbides occur on the austenite grain boundaries.

i Nucleation on dislocations

When a nucleus forms on a dislocation, the Gibbs energy change is not given by (3.14), as the strain energy field associated with the dislocation is locally suppressed [84]. The Gibbs energy change per unit length for a cylinder of radius r forming around the dislocation is:

$$\Delta G = \pi r^2 \Delta G_v + C_{12} - \frac{1}{2} Bb \ln(r) + 2\pi\sigma_{\gamma\theta} r \tag{3.17}$$

where b is the magnitude of the Burgers vector of the dislocation and B a term which depends on its nature (edge, screw or mixed). The solution for $\partial\Delta G/\partial r = 0$, if it exists, is given by:

$$r = \frac{\sigma_{\gamma\theta}}{2\Delta G_v}\left[1 \pm \left\{1 - \frac{\Delta G_v \; Bb^2}{\pi\sigma_{\gamma\theta}}\right\}^{1/2}\right] \tag{3.18}$$

The quantity $\alpha^D = \Delta G_v Bb/(\pi\sigma_{\gamma\theta}^2)$ determines the behaviour of the nucleus: if $\alpha^D > 1$, the energy decreases continuously as the radius increases. If $\alpha^D \leq 1$, there are two solutions and the activation energy G_d^* is the difference between the Gibbs free energy at the two extrema.

The nucleation rate in this case is a function of the dislocation density:

$$I = {N_v}^{1/3} l_d \frac{kT}{h} \exp\left(-\frac{G_d^* + G_t^*}{RT}\right) \tag{3.19}$$

where N_v is the number of atoms per unit volume and l_d is the length of dislocation per unit volume.

ii Grain boundary nucleation

Nucleation on grain boundaries is treated in a similar way: the formation of a nucleus is helped because it suppresses a high energy defect in the crystal. In this case, the

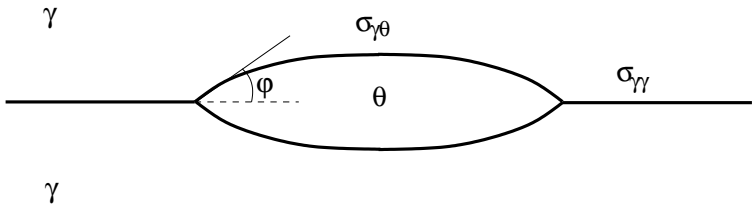

Figure 3.3: Nucleation on a grain-boundary as described by Clemm and Fisher. Adapted from [84].

activation energy is found to be:

$$G_B^* = \frac{4}{27}\frac{\{\eta_{\gamma\theta}\,\sigma_{\gamma\theta} - \eta_{\gamma\gamma}\,\sigma_{\gamma\gamma}\}^3}{\eta_\theta{}^2 \Delta G_v{}^2} \tag{3.20}$$

where $\sigma_{\gamma\gamma}$, $\sigma_{\gamma\theta}$ are the interfacial energies for the grain boundary and the interface precipitate-matrix respectively. $\eta_{\gamma\gamma}$, $\eta_{\gamma\theta}$ are shape factors which relate the area of the interfaces $\gamma\gamma$ and $\gamma\theta$ to the radius of the particle, while η_θ is a shape factor for the volume of the precipitate. In the case described by figure 3.3, they are:

$$\begin{aligned} \eta_\theta &= 2\pi\left(\frac{2 - 3\cos\theta + \cos^2\theta}{3}\right) \\ \eta_{\gamma\gamma} &= \pi \sin^2\theta \\ \eta_{\gamma\theta} &= 4\pi\,(1 - \cos\theta) \end{aligned} \tag{3.21}$$

Johnson *et al.* [85] derived expressions for the activation energy for faceted homogeneous nucleation and for various shapes of grain boundary nucleation. They showed that a change in shape left the critical radius unchanged, but modified the activation energy.

3.2.c The driving force for nucleation

The preceding sections show the need to know the chemical driving force for nucleation ΔG_v. The precipitation of θ in a matrix γ leads to a reduction of Gibbs energy, $\Delta G_\circ$ as illustrated in figure 3.4. The corresponding Gibbs energy change per unit of precipitate is given by $\Delta G_n = \Delta G_\circ / f$ where $f = (\overline{x} - x^{\gamma\theta})/(x^{\theta\gamma} - x^{\gamma\theta})$ is the fraction of precipitate, $\overline{x}$ being the bulk composition (mole fraction), $x^{\gamma\theta}$ the composition of the matrix

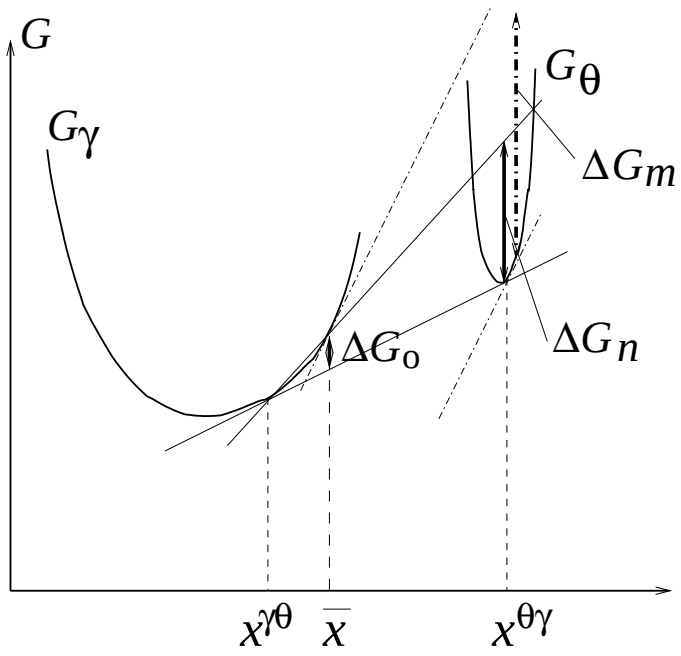

Figure 3.4: An illustration of the construction for finding the driving force for nucleation, $x^{\gamma\theta}$ is mole fraction of solute in the matrix in equilibrium with the precipitate, $\overline{x}$ the bulk mole fraction.

γ in equilibrium with the precipitate θ, and $x^{\theta\gamma}$ the composition of the precipitate θ in equilibrium with the matrix γ. However, the composition of the matrix hardly changes as a consequence of the nucleation, and ΔG_n does not represent correctly the Gibbs energy change during this phenomenon. Furthermore, the composition of the nucleus need not be that corresponding to equilibrium ($x^{\theta\gamma}$), since an alternative composition may lead to a larger Gibbs energy change. The composition that maximises the Gibbs energy change at the nucleation stage is given by the parallel tangent construction [86] as illustrated in figure 3.4. ΔG_m is therefore a better estimate of the driving force for nucleation.

3.3 The growth of precipitates

3.3.a Rate control

The velocity of the interface between matrix and precipitate depends on the mobilities of atoms in the matrix and is related to the atom transfer across the interface. The processes are in series. When the majority of free energy is dissipated in the diffusion of

solute ahead of the interface, the growth is said to be diffusion controlled. It is interface-controlled otherwise. Figure 3.5 illustrates the solute concentration profile in both cases. In the case of diffusion-controlled growth, the interface compositions are given by the

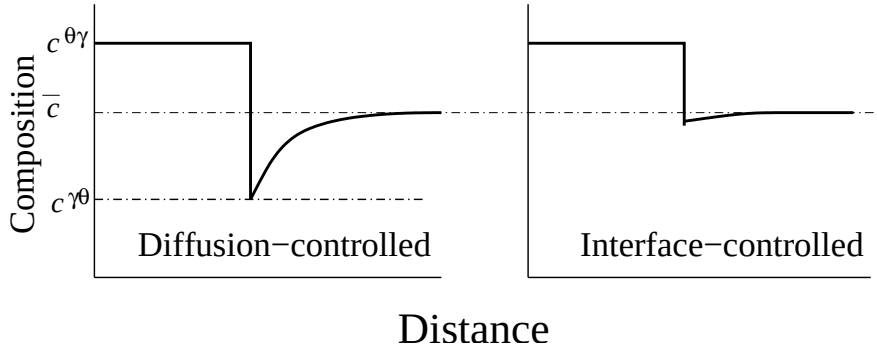

Figure 3.5: Schematic illustration of the solute concentration profile at the interface between the precipitate θ and the matrix γ. $c^{\gamma\theta}$ is the concentration of solute of the matrix in equilibrium with θ, $c^{\theta\gamma}$ that of the precipitate in equilibrium with γ, and $\overline{c}$ is the bulk concentration.

equilibrium phase diagram, as illustrated in figure 4.1.

The following describes, as an example, the Zener model for the growth of a planar interface with a constant far-field concentration ($\overline{c}$), in a binary system. More rigorous models and extension to multicomponent systems are discussed in chapter 4.

3.3.b Zener model for diffusion-control growth

The solute concentration profile at the interface is illustrated in figure 3.5. A simplification introduced by Zener assumes a linear gradient as illustrated in figure 3.6.

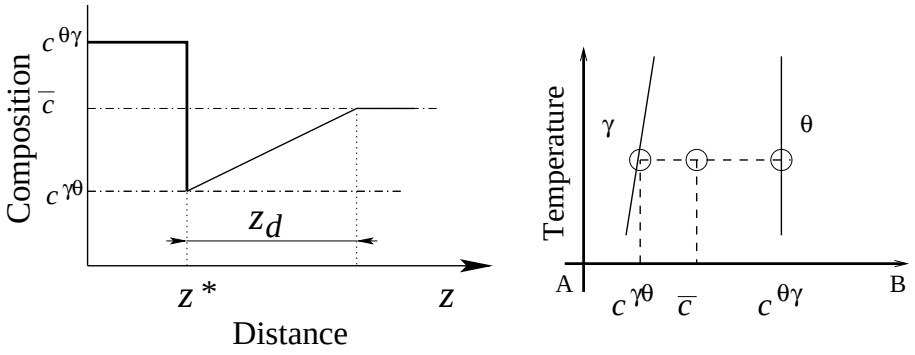

Figure 3.6: The constant concentration gradient approximation [87], and the binary phase diagram showing the composition at the interface $\gamma\theta$.

In this case, the flux of solute arriving at the interface is:

$$J_{z=z^*} = -D \left.\frac{\partial c}{\partial z}\right|_{z=z^*} = -D\frac{\overline{c} - c^{\gamma\theta}}{z_d} \tag{3.22}$$

where z^* is the position of the interface, D the diffusion coefficient of the solute in the matrix, and c the concentration of solute. This flux must equal the rate at which the solute is partitioned:

$$\psi(c^{\theta\gamma} - c^{\gamma\theta}) = |J_{z=z^*}| \tag{3.23}$$

where ψ is the growth rate. z_d can easily be estimated using the mass conservation:

$$\frac{1}{2} z_d(\overline{c} - c^{\gamma\theta}) = z^*(c^{\theta\gamma} - \overline{c}) \tag{3.24}$$

Introducing the dimensionless supersaturation $\Omega = (\overline{c} - c^{\gamma\theta})/(c^{\theta\gamma} - c^{\gamma\theta})$, and combining equations 3.22, 3.23 and 3.24, the velocity is given by:

$$\psi = \frac{\mathrm{d}z^*}{\mathrm{d}t} = \frac{D}{2}\,\Omega\,\frac{\overline{c} - c^{\gamma\theta}}{c^{\theta\gamma} - \overline{c}}\,\frac{1}{z^*} \tag{3.25}$$

Most of the times, it can be assumed that $(c^{\theta\gamma} - \overline{c}) \simeq (c^{\theta\gamma} - c^{\gamma\theta})$, then:

$$\psi = \frac{\mathrm{d}z^*}{\mathrm{d}t} = \frac{D}{2}\Omega^2\frac{1}{z^*} \tag{3.26}$$

Integration leads to:

$$z^* = \Omega\sqrt{Dt} \tag{3.27}$$

The precipitate size therefore varies with the square root of time, giving the classical parabolic law for one-dimensional growth in a binary system.

3.3.c Capillarity effects on the interface compositions

As explained above, in diffusion-controlled growth, the interface compositions are given by the equilibrium phase diagram. However, these diagrams are calculated assuming phases extending indefinitely, that is without surfaces. In the case of precipitation, this is not always a realistic approximation, and the influence of surface energy has to be accounted for.

When a small particle with a curved interface grows, the work done to increase the interface area is not negligible and results in a modification of the expected composition. This is known as the Gibbs-Thomson or *capillarity* effect [84].

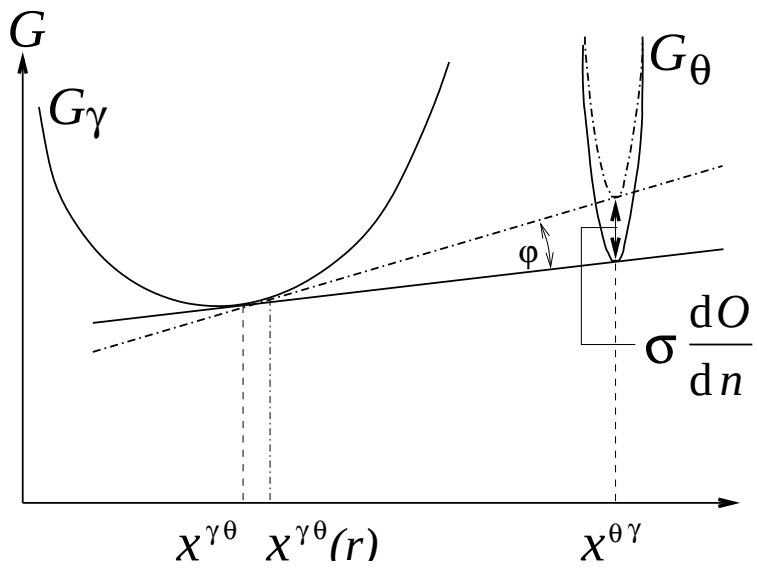

Figure 3.7: Schematic illustration of Gibbs energy and interface composition changes due to the capillarity effect in a binary system. This is a simplified case where the composition of the precipitate is assumed to be constant.

For a curved interface, the increase in Gibbs energy due to the expanding area is given by (figure 3.7), [84]:

$$G_\theta(r) - G_\theta = \sigma_{\theta\gamma}\frac{\mathrm{d}O}{\mathrm{d}n} \tag{3.28}$$

where $\sigma_{\theta\gamma}$ is the energy per unit area of the interface between the matrix and the precipitate, and $\mathrm{d}O/\mathrm{d}n$ is the increase of interface area when a mole of component is transfered to the precipitate.

For a spherical geometry, the term $\mathrm{d}O/\mathrm{d}n$ becomes $2V_m^\theta/r$ where V_m^θ is the molar volume of θ and r the radius of curvature. The calculation of the interface compositions change is given further attention in chapter 5.

3.4 Overall transformation kinetics

As mentioned before, to model multiple precipitation reactions, it is necessary to account for the impingement effects. There are two such effects: *soft-impingement* occurs because of the diffusion fields overlap, while *hard-impingement* is due to contact between the particles.

3.4.a Soft-impingement

In an overall model for precipitation, soft-impingement can be dealt with by using the mean field approximation, in which $\overline{c}$ is not a function of spatial coordinates. It is reduced in agreement with the amount of solute partitioned into the growing precipitates.

Although the validity of this approximation can be discussed when localised precipitation phenomena are dealt with, it is nevertheless extremely useful to avoid recurring to a model requiring spatial coordinates.

3.4.b Hard-impingement: the Avrami equation

We consider the precipitation of θ in a matrix γ, whose initial volume is V. The nucleation and isotropic growth rates, respectively I and ψ are known. The volume of a precipitate nucleated at time τ is, at time t:

$$w_\tau = C\psi^3(t-\tau)^3$$

where C is a shape factor, $4\pi/3$ if the precipitate is spherical.

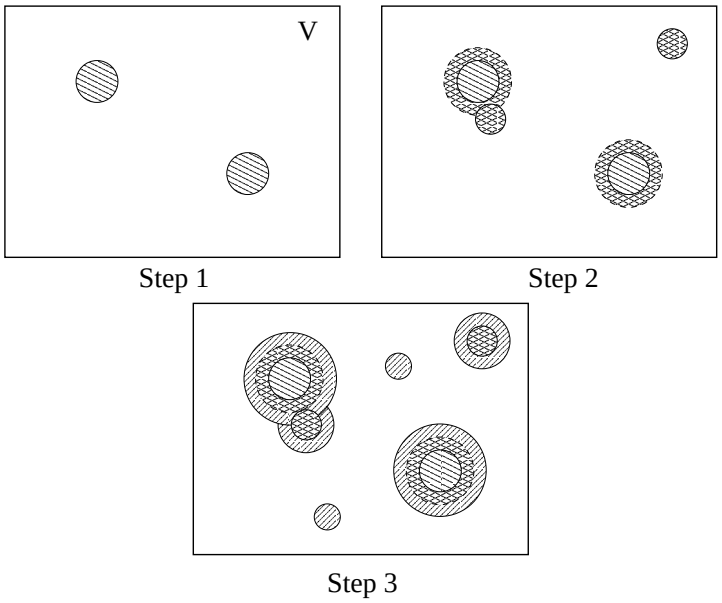

Figure 3.8: The different contributions to the extended volume.

The basic assumption at this stage of the derivation of Avrami's equation is that nucleation and growth occur both in the transformed and untransformed regions, although

it is clear that in reality, neither nucleation nor growth are possible in transformed regions. With this assumption, the number of particles nucleated between τ and $\tau + \mathrm{d}\tau$ is simply $IV\mathrm{d}\tau$, and therefore the contribution of these particles to the total volume of θ at time t is :

$$\mathrm{d}V_\theta^e = w_\tau IV\mathrm{d}\tau$$

The superscript e signifies that this is not a real volume, but an extended volume, because of the assumption made above. The total extended volume is simply the sum of all contributions from particles nucleated between 0 and t:

$$V_\theta^e = \int_{\tau=0}^{t} w_\tau IV\mathrm{d}\tau$$

The change in real volume can be derived by writing:

$$\mathrm{d}V_\theta = \left(1 - \frac{V_\theta}{V}\right)\ \mathrm{d}V_\theta^e$$

i.e. the change in real volume is the proportion of the change in extended volume which occurred in the untransformed volume. Assuming I and ψ to be independent of time, an analytical solution for the volume fraction of θ is immediately derived:

$$V_f(\theta) = 1 - \exp\left(-\frac{CI\psi^3 t^4}{4}\right)$$

3.4.c Modification for simultaneous reactions

Obviously, the Avrami equation as introduced above is only able to deal with a single reaction, or a succession of independent reactions. This is not satisfying for the description of multiple precipitation reactions which clearly interact with each other, by competing for solute and nucleation sites. Robson and Bhadeshia [88] proposed a modification of this equation as follows.

If two phases θ and γ can form from a volume V of γ with different growth and nucleation rates, we still can write the contribution of the ones nucleated between τ and $\tau + \mathrm{d}\tau$ as:

$$\begin{aligned} \mathrm{d}V_\theta^e &= C\psi_\theta^3 I_\theta V(t-\tau)^3\mathrm{d}\tau \\ \mathrm{d}V_\gamma^e &= C\psi_\gamma^3 I_\gamma V(t-\tau)^3\mathrm{d}\tau \end{aligned} \qquad (3.29)$$

but when correcting for the extended volume:

$$\mathrm{d}V_\theta = \left(1 - \frac{V_\theta + V_\gamma}{V}\right) \mathrm{d}V_\theta^e$$
$$\mathrm{d}V_\gamma = \left(1 - \frac{V_\theta + V_\gamma}{V}\right) \mathrm{d}V_\gamma^e$$

The extension to multiple reactions is immediate:

$$\mathrm{d}V_j = \left(1 - \frac{\sum_i V_i}{V}\right) \mathrm{d}V_j^e \tag{3.30}$$

However, such systems have no general analytical solution if no relationship is assumed between the parameters of the two phases (nucleation and growth rates).

3.5 Summary

The CALPHAD method, which is at the heart of the prediction of the phase behaviour of complex systems, has been presented briefly, together with the format of the SGTE databases used with most thermodynamic calculation packages such as MT-DATA or ThermoCalc.

Physical models for nucleation and growth of a single particle rely on the availability of thermodynamic information such as the Gibbs energy change during precipitation, or the equilibrium interface composition. Simple models have been presented for nucleation and growth, the latter being given more attention in chapter 4.

The overall precipitation phenomenon cannot be modelled accurately without accounting for interactions between the different particles. Soft-impingement can be dealt with using the mean-field approximation while the concept of extended volume, modified for multiple precipitation reactions, provides a solution to the hard-impingement problem.